THE JOURNAL OF PHYSICAL CHEMISTRY B LETTERS

2005, *109,* 16563−16566
Published on Web 08/12/2005

Spectroscopic Identification of the Reaction Intermediates in Oxygen Reduction on Gold in Alkaline Solutions

M. H. Shao and R. R. Adzic*

Department of Materials Science, Brookhaven National Laboratory, Upton, New York 11973

Received: June 24, 2005; In Final Form: July 25, 2005

Surface enhanced infrared reflection−absorption spectroscopy with an attentuated total reflection configuration (ATR-SEIRAS) was used for the first time to identify the intermediates of the oxygen reduction reaction (ORR) on gold electrodes. Our study employed a Au thin-film electrode in acidic and alkaline solutions. In alkaline solutions, a potential dependent band at 1268 cm^{-1}, which we assigned to the antisymmetric bending mode of OOH of adsorbed HO_2^-, was observed between 0.1 and −0.6 V versus Ag|AgCl, Cl^-, exactly in the potential range where the ORR occurred. The assignment was supported by our isotope exchange experiment. The adsorbed HO_2^- is a reaction intermediate in the $4e^-$ serial mechanism. In acidic solutions, there was only a very weak band at the same position, reflecting the fast protonation of HO_2^-. This finding may imply that the interaction between HO_2^- and Au surfaces is very weak in acidic solutions, in agreement with the observed $2e^-$ reduction mechanism.

1. Introduction

The oxygen reduction reaction (ORR) is of paramount importance for electrochemical energy conversion systems, such as fuel cells and corrosion processes.[1] It represents a major problem in electrocatalysis and fuel cell technology because of its slow kinetics and the large Pt content required in existing electrocatalysts.[1,2]

The ORR on gold has been studied extensively both in acidic and in alkaline solutions.[3−16] These works showed that the pathway of the ORR on Au depended on the electrode's potential, surface structure, and pH.[1,9,10,12,13] In acidic solutions, a $2e^-$ pathway yielding hydrogen peroxide as the final product was dominant, independent of the electrode's surface structure.[9] In alkaline solutions, a $4e^-$ pathway was observed on Au(100) and vicinal faces in a certain potential range;[8,10−12,14] these findings were explained by the presence of highly discharged adsorbed OH^- acting as a precursor of oxygen intermediates[13] or by specific interactions between the hydrogen peroxide anions and Au surfaces.[15] Despite numerous investigations, the detailed mechanism of the ORR still is unclear. Superoxide (O_2^-) and hydrogen peroxide anions (HO_2^-) were proposed as the adsorbed reaction intermediates in the ORR.[1,3,17] However, due to the short lifetime of the intermediates, and their weak interactions with the electrode surfaces, their in situ identification defied almost all attempts using spectroscopic techniques in usual aqueous solutions. Very recently, Li and Gerwirth[18] observed adsorbed superoxide anions at 1165 cm^{-1} as a reaction intermediate in the ORR on bare and Bi-modified Au electrodes in acidic solution by surface enhanced Raman scattering (SERS), though no further identification of this band was made. Wu et al.,[19] measuring the charge associated with adsorbed intermediates on Au in KOH solution by rotating disk electrode-potential step coulometry, found indications of the existence of adsorbed HO_2^-. However, this technique is not species specific.

Surface enhanced infrared reflection−absorption spectroscopy with attenuated total reflection (ATR-SEIRAS) was shown to be a powerful technique for studying solid−liquid interfaces.[20−22] The vibration signals from the adsorbates on a working electrode are enhanced remarkably, while the interference from the background is minimized.[20,21] In addition, there are no severe transport limitations for reactants, as in infrared reflection−absorption spectroscopy (IRRAS). Accordingly, we took advantage of ATR-SEIRAS methodology to identify the adsorbed intermediates in the ORR on Au.

2. Experimental Section

The general details of the Fourier transform infrared spectroscopy with attenuated total reflection (ATR-FTIR) experiments are described elsewhere.[20−23] In brief, we employed a fast-scan Nicolet Nexus 670 FTIR spectrometer equipped with a mercury cadmium telluride (MCT) detector cooled with liquid nitrogen to record FTIR spectra without using polarization discrimination. The spectral resolution was set to 8 cm^{-1}, and 54 interferograms were coadded to each spectrum. Spectra are given in absorbance units defined as $A = -\log(R/R_0)$, where R and R_0 represent the reflected IR intensities corresponding to the sample and reference single-beam spectra, respectively. All of the experiments were carried out at room temperature (∼20 °C).

A hemispherical polycrystalline Si crystal, 2.54 cm in diameter, was used as the internal reflection element (IRE), as well as the Au deposition substrate. Before electroless deposition of Au, the surface for IR reflection was polished with alumina powder, using 0.05 μm grade for the final polishing. The Si oxide film was removed with a dilute HF solution (10%) before

* To whom correspondence should be addressed. E-mail: adzic@bnl.gov. Phone: +1-631-344-4522. Fax: +1-631-344-5815.

10.1021/jp053450s CCC: $30.25

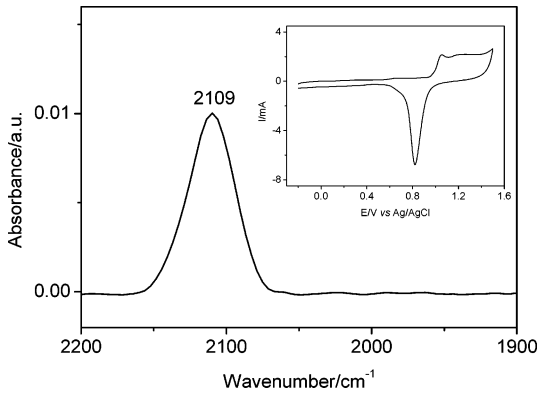

Figure 1. SERIA spectrum of CO absorbed on a Au thin-film electrode in 0.1 M $HClO_4$ at −0.1 V. The reference spectrum was taken in the same solution without CO at −0.1 V. The inset is a typical cyclic voltammogram for the Au thin-film electrode on a Si hemisphere in 0.1 M $HClO_4$ solution at a scan rate of 100 mV s^{-1}.

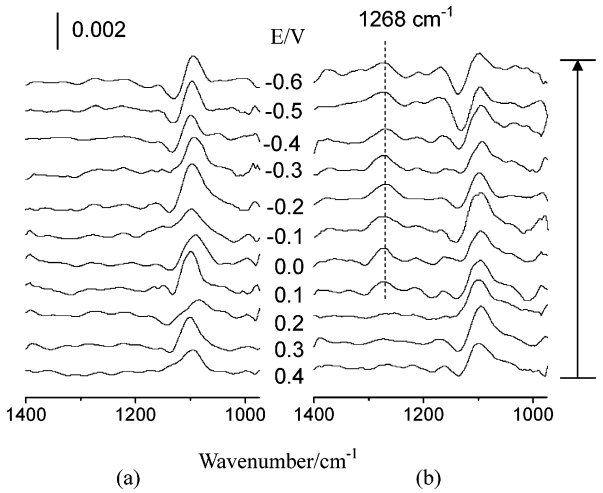

Figure 2. SERIA spectra in the range 1400−975 cm^{-1} recorded for the Au thin-film electrode in (a) nitrogen- and (b) oxygen-saturated 0.1 M $NaClO_4$ solution (pH 0) during the cathodic scan at a scan rate of 5 mV s^{-1}. The reference spectra were taken at 0.4 V before the potential scans started.

exposing the IRE's flat surface to the plating solution. Afterward, the remaining Si surface was terminated by hydrogen to improve the adhesion between the substrate and Au film.[24] The plating solution (0.02 M $HAuCl_4 \cdot xH_2O$ + 1.5% HF) was left on the treated surface for 4 min at room temperature. The deposition mechanism, which involves the discharge of $AuCl_4^-$ and the formation of SiF_6^{2-}, was described elsewhere.[24,25] Compared with other deposition procedures,[24] the one we used does not need a high temperature and its composition is simpler. The Au thin film thus formed was rinsed with a plentiful amount of Milli-Q UV plus water and then attached to a three-electrode spectro-electrochemical cell with an ultrathin Au foil connecting the working electrode to a CHI604A electrochemical analyzer (CH Instruments). A Pt ring and an Ag|AgCl, Cl^- electrode were used as the counter and reference electrode, respectively. The potentials in this paper are expressed with respect to this reference electrode. The electrolytes were 0.1 M $HClO_4$ and 0.1 M $NaClO_4$, saturated with nitrogen or oxygen. The pH of the $NaClO_4$ solution was adjusted by adding NaOH. Before measurements, the as-grown Au film was cycled in 0.1 M $HClO_4$ between −0.1 and 1.5 V until stable voltammetry curves were obtained.

Aldrich was the supplier of D_2O with 99.9 atom % D isotope purity. Before the injection of D_2O solution into the spectro-electrochemical cell, the Au thin film was dried with dry nitrogen to eliminate adsorbed H_2O moisture on its surface.

3. Results and Discussion

3.1. Characterization of the Au Thin-Film Electrode. The inset in Figure 1 shows a typical cyclic voltammogram for the Au thin-film electrode in 0.1 M $HClO_4$ solution. The curve is similar to that of polycrystalline Au.[26] The film's roughness factor was about 5. It was obtained by comparing the integrated charge density for oxide reduction with the theoretical value of 480 μC cm^{-2} required for reducing a monolayer of Au oxide.[27]

The surface-enhancement effect of the Au film electrode was examined by CO adsorption. The electrode was kept in CO-saturated 0.1 M $HClO_4$ solution at −0.1 V for 5 min to ensure that a CO adlayer formed on the Au surface; then, the solution was purged with nitrogen gas to remove the dissolved CO. Figure 1 shows a spectrum in the range of CO adsorption recorded at −0.1 V. The reference spectrum was taken at the same potential before bubbling with CO. Only a strong band at 2109 cm^{-1} is present. A linearly bonded CO band (υ_{CO}) was apparent at around 2100 cm^{-1} on both the polycrystalline and single-crystal Au surfaces.[24,26,28] Thus, the band shown in Figure 1 can be assigned to υ_{CO}. Compared with the data from IRRAS,[28] the band intensity of υ_{CO} here is about 20 times larger. Moreover, the interference from Au-silicide is negligible, since no band due to CO adsorbed on silicide is observed in our spectra, which should appear at 2030 cm^{-1}.[26] As interpreted by Osawa, a nearly continuous Au film separated the Au nanoparticles and Si substrate,[24] which prevented the direct exposure of silicide to the electrolyte.

3.2. Oxygen Reduction on Au Thin-Film Electrodes. Figure 2a shows a series of SEIRA spectra between 1400 and 975 cm^{-1} recorded in the cathodic scan for the Au thin-film electrode in a nitrogen-saturated 0.1 M $NaClO_4$ solution (pH 9). The reference spectrum was taken at 0.4 V in the same solution before the potential scan started. Only a broad band around 1100 cm^{-1} is present in the whole potential range. We note that the background spectrum has a sharp edge at ∼1100 cm^{-1} (not shown here) caused by the strong IR absorption of Si.[29] Thus, this band may be induced by the interference from Si. In the oxygen-saturated solution (Figure 2b), an additional band at 1268 cm^{-1} begins to appear at 0.1 V, where the ORR starts. This band is present at all potentials between 0.1 and −0.6 V. Figure 3 shows the change of integrated band area as a function of potential. The band's intensity reaches a maximum at −0.2 V and then decreases gradually as the potential approaches more negative values. The difference in the FTIR spectra between Figure 2a and b indicates that the band at 1268 cm^{-1} is due to an oxygen-associated species.

To analyze the origin of this band further, similar FTIR experiments were conducted with D_2O as the solvent, instead of H_2O. Figure 4 shows the SEIRA spectra recorded in the cathodic scan for the Au thin-film electrode in oxygen-saturated 0.1 M $NaClO_4$ + D_2O solution (pD 6). There is no band in the range 1300−1200 cm^{-1}. However, in the oxygen-saturated 0.1 M $NaClO_4$ + H_2O solution (pH 6), a band exists at 1268 cm^{-1} (not shown here). These results suggest that hydrogen atom also is involved in the vibration mode at 1268 cm^{-1}.

The υ_6 band (antisymmetric bending mode of OOH) of hydrogen peroxide at 1260−1280 cm^{-1} is known to be much stronger than its other vibrational bands, except υ_4 at 317 cm^{-1}.[30−33] For instance, the intensity of υ_6 is about 600 times larger than that of υ_3 (O−O stretching mode) at 860 cm^{-1}.[30]

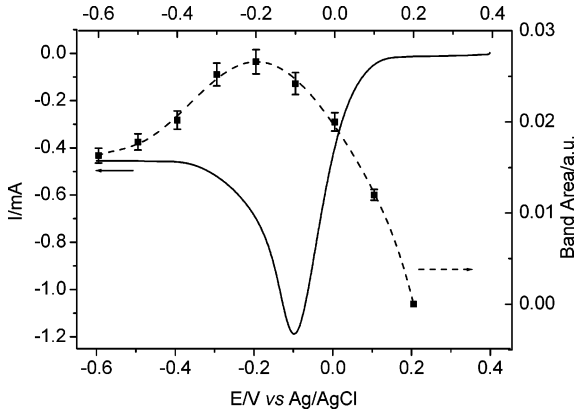

Figure 3. Potential dependence of the integrated band areas for the antisymmetric bending mode of OOH for O_2 reduction on Au in 0.1 M $NaClO_4$ (dashed line with square symbols). The solid line shows the corresponding voltammogram of the ORR at a scan rate of 5 mV s^{-1}.

Thus, we tentatively assign this band to the antisymmetric bending of OOH of the adsorbed hydrogen peroxide anion, HO_2^-. This assignment also is consistent with the OOH bending mode of TiOOH reported by Nakamura et al.[34] In D_2O solution, the OOD bending mode may downshift below 1000 cm^{-1}, which is beyond our system's detection limit. This large shift in frequency is not surprising, according to the reported data. The redshift of the OOH bending mode in the H−D isotope effect is about 290 and 320 cm^{-1} for the H_2O_2-to-HDO_2 and H_2O_2-to-D_2O_2 changes, respectively.[33] An ∼300 cm^{-1} redshift also was observed from TiOOH to TiOOD.[34]

We also conducted the SEIRAS experiment in oxygen-saturated 0.1 M $HClO_4$ solution. A much weaker band at the same position is observed in the ORR in a considerably narrower potential range (not shown).

The ORR on Au in acidic media is a $2e^-$ process, generating hydrogen peroxide as the only final product on all faces. In alkaline media, however, the surface orientation dependent reaction mechanisms were found, as summarized in the Introduction. Below, we show a simplified scheme for the ORR on Au in alkaline solutions involving a serial pathway; this depiction is based on one segment of Anastasijevic et al.'s general scheme[1,17] and on one feature (k_5) of the scheme by Wroblowa et al.:[3]

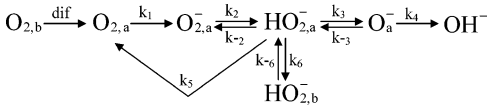

The subscripts a and b denote the adsorbed and bulk species, respectively. In a serial pathway, the first electron transfer is usually considered to be the rate-determining step (k_1) on several surfaces producing adsorbed superoxide anions, followed by the protonation to form hydrogen peroxide anions (k_2):[1,13]

$$O_{2,a} + e^- \rightarrow O_{2,a}^- \quad (1)$$

$$O_{2,a}^- + H_2O + e^- \rightarrow HO_2^- + OH^- \quad (2)$$

The two events may occur simultaneously.[1] In our SEIRAS data, no band could be attributed to superoxide anion, which was observed by Li et al.[18] and Brooker et al.[35] This can be due to the very short lifetime of this species and the interference from Si background at ∼1100 cm^{-1}. Nevertheless, the spectra clearly show that HO_2^- is the reaction intermediate in alkaline media,

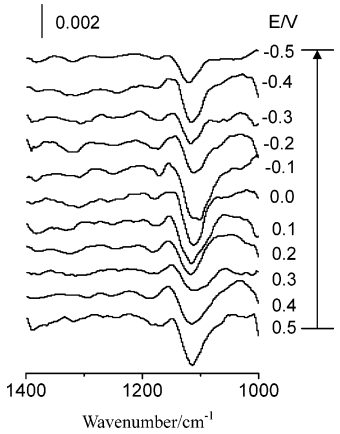

Figure 4. SEIRA spectra in the range 1400−1000 cm^{-1} recorded for the Au thin-film electrode in oxygen-saturated 0.1 M $NaClO_4$ + D_2O solution (pD 6) during the cathodic scan at a scan rate of 5 mV s^{-1}. The reference spectrum was taken at 0.5 V before the potential scan started.

in good agreement with the literature, wherein the adsorbed HO_2^- was derived on the basis of the rotating disk-ring electrode[4] and rotating disk electrode-potential step coulometry measurements.[19] At active surfaces, such as Au(100), HO_2^- can be further reduced to OH^-, resulting in a $4e^-$ serial pathway:[12,17]

$$HO_2^- + 2e^- + H_2O \rightarrow 3OH^- \quad (3)$$

The spectra indicate that the adsorption of HO_2^- occurs when the ORR starts. In the diffusion-controlled region (between −0.2 and −0.6 V), the coverage of HO_2^- decreases due to the weaker interaction between Au surfaces and HO_2^-, even though more HO_2^- anions are produced, since a quantitative $2e^-$ pathway occurs at most faces in this region. Previous studies of the ORR on Au(*hkl*) in alkaline media revealed that only Au(100) and its vicinal faces exhibited a $4e^-$ serial pathway in the mixed control region.[6,10] Thus, only the fraction of Au nanoparticle film with the (100) face may contribute to the observed adsorption of HO_2^- in this case, since the interactions between HO_2^- and other faces are too weak. The large current peak in Figure 3 indicates the 4e reduction of O_2, that is, the pronounced presence of the (100) orientation. However, the presence of HO_2^- on other faces cannot be completely ignored.

In acidic solutions, the protonation of $O_{2,a}^-$ and $HO_{2,a}^-$ is much faster than that in alkaline solutions, leading to the formation of H_2O_2, which easily leaves the surface:

$$HO_2^- + H^+ \rightarrow H_2O_2 \quad (4)$$

This may explain why the observed band associated with HO_2^- is much weaker in 0.1 M $HClO_4$. This much weaker interaction between the Au surface and reaction intermediate (HO_2^-) agrees well with the $2e^-$ mechanism of the ORR in acidic media.[9]

4. Conclusions

We studied the ORR on an Au thin-film electrode in situ by the ATR-SEIRAS technique, both in acidic and in alkaline solutions. In alkaline solutions, a potential dependent band at 1268 cm^{-1} is present between 0.1 and −0.6 V, where the ORR takes place. We assigned this band to the antisymmetric bending mode of OOH of adsorbed HO_2^-, which was proposed as one of the adsorbed reaction intermediates in previous studies. Since only the (100) face exhibits the $4e^-$ serial mechanism, a specific

interaction between HO_2^- and the (100) face must exist, and most of the HO_2^- was believed to be adsorbed on the (100) face. In acidic solution, the protonation of $O_{2,a}^-$ and $HO_{2,a}^-$ is much faster, so that only a very weak band is seen at the same position. This implies that the interaction between HO_2^- and Au surfaces is very weak in acid, a finding that provides support for previous assumptions about this adsorbate.

Acknowledgment. This work is supported by US Department of Energy, Divisions of Chemical and Material Sciences, under Contract No. DE-AC02-98CH10886. The authors appreciate the valuable discussions with N. S. Marinkovic and J. X. Wang. M.H.S. acknowledges partial support from Department of Materials Science and Engineering, State University of New York at Stony Brook.

References and Notes

(1) Adzic, R. R. In *Electrocatalysis*; Lipkowski, J., Ross, P. N., Eds.; Wiley: New York, 1998.

(2) Gottesfeld, S.; Zawodzinski, T. A. In *Advances in Electrochemical Science and Engineering*; Alkire, R. C., Kolb, D. M., Eds.; Wiley: Weinheim, Germany, 1997; Vol. 5.

(3) Wroblowa, H. S.; Pan, Y.-C.; Razumney, G. *J. Electroanal. Chem.* **1976**, *69*, 195.

(4) Zurila, R. W.; Sen, R. K.; Yeager, E. *J. Electrochem. Soc.* **1978,** *125*, 1103.

(5) Fisher, P.; Heitbaum, J. *J. Electroanal. Chem.* **1980**, *112*, 231.

(6) Adzic, R. R.; Markovic, N. M.; Vesovic, V. B. *J. Electroanal. Chem.* **1984**, *165*, 105.

(7) Markovic, N. M.; Adzic, R. R.; Vesovic, V. B. *J. Electroanal. Chem.* **1984**, *165*, 121.

(8) Anastasijevic, N. A.; Strabac, S.; Adzic, R. R. *J. Electroanal. Chem.* **1988**, *240*, 239.

(9) Adzic, R. R.; Strabac, S.; Anastasijevic, N. A. *Mater. Chem. Phys.* **1989**, *22*, 349. Strabac, S.; Adzic, R. R. *J. Serb. Chem. Soc.* **1992**, *57*, 835.

(10) Strabac, S.; Anastasijevic, N. A.; Adzic, R. R. *J. Electroanal. Chem.* **1992**, *323*, 179.

(11) Strabac, S.; Adzic, R. R. *Electrochim. Acta* **1994**, *39*, 983.

(12) Strabac, S.; Adzic, R. R. *Electrochim. Acta* **1996**, *41*, 2903.

(13) Strabac, S.; Adzic, R. R. *J. Electroanal. Chem.* **1996**, *403*, 169.

(14) Schmidt, T. J.; Stamenkovic, V.; Arenz, M.; Markovic, N. M.; Ross, P. N. *Electrochim. Acta* **2002**, *47*, 3765.

(15) Prieto, A.; Hernandez, J.; Herrero, E.; Feliu, J. M. *J. Solid State Electrochem.* **2003**, *7*, 599.

(16) Blizanac, B. B.; Lucas, C. A.; Gallagher, M. E.; Arenz, M.; Ross, P. N.; Markovic, N. M. *J. Phys. Chem. B* **2004**, *108*, 625.

(17) Anastasijevic, N. A.; Vesovic, V.; Adzic, R. R. *J. Electroanal. Chem.* **1987**, *229*, 305.

(18) Li, X.; Gewirth, A. A. *J. Am. Chem. Soc.* **2005**, *127*, 5252.

(19) Wu, B.-l.; Lei, H.-w.; Cha, C.-s.; Chen, Y.-y. *J. Electroanal. Chem.* **1994**, *377*, 227.

(20) Ataka, K.; Yotsuyanagi, T.; Osawa, M. *J. Phys. Chem.* **1996**, *100*, 10664. Osawa, M. *Bull. Chem. Soc. Jpn.* **1997**, *70*, 2861. Miki, A.; Ye, S.; Osawa, M. *Chem. Commun.* **2002**, *14*, 1500. Chen, Y. X.; Miki, A.; Ye, S.; Sakai, H.; Osawa, M. *J. Am. Chem. Soc.* **2003**, *125*, 3680. Yajima, T.; Uchida, H.; Watanabe, M. *J. Phys. Chem. B* **2004**, *108*, 2654. Wandlowski, T.; Ataka, K.; Pronkin, S.; Diesing, D. *Electrochim. Acta* **2004**, *49*, 1233.

(21) Shao, M. H.; Adzic, R. R. *Electrochim. Acta* **2005**, *50*, 2415.

(22) Shao, M. H.; Warren, J.; Marinkovic, N. S.; Faguy, P. W.; Adzic, R. R. *Electrochem. Commun.* **2005**, *7*, 459.

(23) Faguy, P. W.; Marinkovic, N. S. *Appl. Spectrosc.* **1996**, *50*, 394.

(24) Miyake, H.; Ye, S.; Osawa, M. *Electrochem. Commun.* **2002**, *4*, 973.

(25) Nagahra, L. A.; Ohmori, T.; Hashimoto, K.; Fujishima, A. *J. Electroanal. Chem.* **1992**, *333*, 363. Kuznetsov, G. V.; Skryshevsky, V. A.; Vdovenkova, T. A.; Tsyganova, A. I.; Gorostiza, P.; Sanz, F. *J. Electrochem. Soc.* **2001**, *148*, C528.

(26) Sun, S.-G.; Cai, W.-B.; Wan, L.-J.; Osawa, M. *J. Phys. Chem. B* **1999**, *103*, 2460.

(27) Oesch, U.; Janata, J. *Electrochim. Acta* 1983, 28, 1247. Zhang, Y.; Asahina, S.; Yoshihara, S.; Shirakashi, T. *Electrochim. Acta* **2003**, *48*, 741.

(28) Chang, S.-C.; Hamelin, A.; Weaver, M. J. *Surf. Sci.* **1990**, *239*, L543. Chang, S.-C.; Hamelin, A.; Weaver, M. J. *J. Phys. Chem.* **1991**, *95*, 5560.

(29) Kataoka, S.; Tejedor-Tejedor, M. I.; Coronado, J. M.; Anderson, M. A. *J. Photochem. Photobiol., A* **2004**, *163*, 323.

(30) Rogers, J. D.; Hillman, J. J. *J. Chem. Phys.* **1981**, *75*, 1085.

(31) Rogers, J. D.; Hillman, J. J. *J. Chem. Phys.* **1981**, *76*, 4046.

(32) May, R. D. *J. Quant. Spectosc. Radiat. Transfer* **1991**, *45*, 267.

(33) Pettersson, M.; Tuominen, S.; Rasanen, M. *J. Phys. Chem. A* **1997**, *101*, 1166. Engdahl, A.; Nelander, B.; Karlstrom, G. *J. Phys. Chem. A* **2001**, *105*, 8393.

(34) Nakamura, R.; Imanishi, A.; Murakoshi, K.; Nakato, Y. *J. Am. Chem. Soc.* **2003**, *125*, 7443.

(35) Brooker, J.; Christensen, P. A.; Hamnett, A.; He, R.; Paliteiro, C. A. *Faraday Discuss.* **1992**, *94*, 339.